J. Phys. B: At. Mol. Opt. Phys. **29** (1996) 4285–4301. Printed in the UK

A distorted-wave study of electronic excitation to some low-lying states of CO by electron impact

M-T Lee†, A M Machado‡, M M Fujimoto†, L E Machado‡ and L M Brescansin‡§

† Departamento de Química, Universidade Federal de São Carlos, 13565-905, São Carlos, SP, Brazil

‡ Departamento de Física, Universidade Federal de São Carlos, 13565-905, São Carlos, SP, Brazil

§ Instituto de Física 'Gleb Wataghin', UNICAMP, 13083-970, Campinas, SP, Brazil

Received 29 May 1996, in final form 10 July 1996

Abstract. The distorted-wave approximation is applied to study electron-impact excitation leading to the a $^3\Pi$, b $^3\Sigma^+$, A $^1\Pi$ and B $^1\Sigma^+$ states of CO in the 20–100 eV range. Our calculated DCS and ICS are compared with available theoretical and experimental data. In general our cross sections are in quite good agreement with previous two- and five-state Schwinger multichannel results. Also, good qualitative agreement with the experimental data is obtained. However, in general our theory overestimates the cross sections. In comparison with a previous DWA study, our work reveals the strong influence of the description of the target wavefunctions on the calculated cross sections.

1. Introduction

Electronic excitation cross sections of atoms and molecules are of fundamental importance in a great variety of physical and chemical processes and constitute a subject of continuously increasing interest to both experimentalists and theoreticians working in this field (Trajmar *et al* 1983). However, both the measurements and the *ab initio* calculations of such cross sections are, in general, difficult and up until now only a few results have been reported in the literature. Also, discrepancies are frequently found among various data (Trajmar *et al* 1983, Collins and Schneider 1990). So, the search for theoretical computationally 'affordable' methods that can provide reliable cross sections is highly desirable and comparative studies among several theoretical methods are clearly of interest.

Over the past two decades several low-order theories such as the Born and Ochkur-Rudge approximations (Cartwright and Kuppermann 1967, Chung *et al* 1975, Chung and Lin 1974), the impact-parameter method (Hazi 1981), and distorted-wave approximations (DWA, Rescigno *et al* 1974, Fliflet and McKoy 1980, Lee and McKoy 1982, Lee *et al* 1990a, b, 1991) have been applied to the inelastic electron scattering associated with the electronic excitation of molecules. These theories are relatively easy to apply and can provide useful results in some applications. In particular, the DWA (Bartschat and Madison 1987) and first-order many-body theory (FOMBT, Meneses *et al* 1990), which is essentially equivalent to DWA, have been widely applied to calculate electronic excitation cross sections and coherence parameters for atomic targets in the intermediate and high energy range. Earlier calculations in H_2 (Lee *et al* 1990a, 1996) suggested that the DWA could be adequate for

0953-4075/96/184285+17$19.50

studies of molecular electronic excitation by electron impact in the intermediate energy range. Nevertheless, no such systematic comparative studies have so far been reported for other molecular targets. Among the systems of interest is the CO molecule, one of the most important constituents of the Earth's atmosphere, as well as of interestellar matter. Excitation and dissociation of CO by photon and electron collisions are relevant for the interpretation of emission spectra and for the understanding of the detailed energy flow and chemistry in these media (Fox and Dalgarno 1979, Cooper and Kirby 1987). Also, the knowledge of cross sections for electron-collision processes involving CO is particularly important to the study of plasmas and electric discharges (McDaniel and Nighan 1982).

Recently, experimental differential cross sections (DCS) for electronic excitation to several low-lying states of CO in the energy range 20–50 eV have been reported (Middleton *et al* 1993, Middleton 1994). Integral cross sections for the excitation of the a $^3\Pi$ state of CO by electron impact in the energy range from threshold up to 50 eV were measured by LeClair *et al* (1994) and up to 70 eV by Furlong and Newell (1996). Cross sections for excitations leading to the B $^1\Sigma^+$, C $^1\Sigma^+$ and E $^1\Pi$ states at 100 eV have also been measured by Kanik *et al* (1993). Calculations of excitation cross sections in the low-incident energy range (from threshold up to 30 eV) were reported by Weatherford and Huo (1990) and by Sun *et al* (1992) using the Schwinger multichannel method (SMC), and by Morgan and Tennyson (1993) using the *R*-matrix method. Comparison with these data can provide more information about the applicability of the distorted-wave method in the calculation of molecular excitation cross sections.

In this paper, we report distorted-wave cross sections for the transitions leading to the a $^3\Pi$, b $^3\Sigma^+$, A $^1\Pi$ and B $^1\Sigma^+$ states of CO by electron impact at incident energies ranging from 20 to 100 eV. Distorted-wave studies for some of these transitions had been carried out previously by Lee and McKoy (1982) in the 20–50 eV range. In the present DWA study we have improved the description of both the ground and the excited states of the target, as well as the convergence of the partial-wave expansions of the electron continuum wavefunction. As we will show below, these improvements are important in the excitations to the a $^3\Pi$ and A $^1\Pi$ states, particularly at low incident energies. In addition, the DCS for the X $^1\Sigma^+ \rightarrow$ B $^1\Sigma^+$ transition and those at energies above 50 eV for all transitions are reported here for the first time.

The organization of this paper is as follows. In section 2 we briefly outline the theory used, in section 3 we present some computational details and in section 4 we discuss our results. Finally, in section 5 we summarize our conclusions.

2. Theory

The details of the basic theory used in this work have already been presented elsewhere (Rescigno *et al* 1974, Fliflet and McKoy 1980, Lee and McKoy 1982, Lee *et al* 1990a, b, 1991) and will be only briefly described here. Excitation DCS for electron–molecule scattering averaged over the molecular orientations are given by

$$\frac{\mathrm{d}\sigma}{\mathrm{d}\Omega} = SM_f \frac{k_f}{k_\mathrm{i}} \frac{1}{8\pi^2} \int \mathrm{d}\alpha \sin\beta \,\mathrm{d}\beta \,\mathrm{d}\gamma \,|f(\hat{k}'_f)|^2 \tag{1}$$

where the S factor results from summing over the final and averaging over the initial spin sublevels, M_f is the orbital angular momentum projection degeneracy factor of the final target state, $f(\hat{k}'_f)$ is the laboratory-frame (LF) scattering amplitude, $\boldsymbol{k}'_f$ ($\boldsymbol{k}'_i$) is the scattered (incident) electron linear momentum in LF. The direction of the incident electron linear momentum is taken as the LF z-axis in our study and (α, β, γ) are the Euler angles

which define the direction of the molecular principal axis. The body-frame (BF) scattering amplitude $f(\hat{k}_f, \hat{k}_i)$ is related to the T-matrix elements by the formula

$$f(\hat{k}_f, \hat{k}_i) = -2\pi^2 T_{fi} \,. \tag{2}$$

According to the two-potential formalism, if the exact interaction potential operator is split into

$$V = V_1 + V_2 \tag{3}$$

the exact transition matrix, T_{fi}, can be written as

$$T_{fi} = \langle \Phi_f \mid U_1 \mid \chi_i^+ \rangle + \langle \chi_f^- \mid U_2 \mid \Psi_i^+ \rangle \tag{4}$$

where $U_i = 2V_i$ is the reduced potential operator in atomic units. In equation (4) Ψ is the exact solution for the (e^- + molecule) system, χ is the distorted-wave solution and Φ is the unperturbed solution. They satisfy the corresponding Schrödinger equations,

$$(H_0 + V - E)\Psi = 0 \tag{5}$$

$$(H_0 + V_1 - E)\chi = 0 \tag{6}$$

and

$$(H_0 - E)\Phi = 0 \tag{7}$$

where $H_0 = H_M - \frac{1}{2}\nabla^2$ is the unperturbed Hamiltonian operator for the system and H_M is the Hamiltonian operator for an isolated molecule.

In principle, the choice of V_1 is arbitrary. In this study, the distorted wavefunctions for both the incident and the scattered electrons are calculated in the static-exchange (SE) potential generated by the ground-state target. This particular choice of V_1 makes our DWA equivalent to FOMBT and, according to Rescigno *et al* (1974), the most important effects for non-resonant scattering are incorporated in this formalism. The resulting DWA transition matrix is given by

$$T_{fi} = \langle \mathcal{A}(\varphi_1 \chi_{\boldsymbol{k}_f}^-) \mid U_2 \mid \mathcal{A}(\varphi_0 \chi_{\boldsymbol{k}_i}^+) \rangle \tag{8}$$

where $\mathcal{A}$ is the antisymmetrizer operator, φ_0 and φ_1 are the initial and the final one-determinant target wavefunctions, respectively, and $\chi_{\boldsymbol{k}_i}^+$ and $\chi_{\boldsymbol{k}_f}^-$ are the initial and the final one-electron distorted continuum wavefunctions. φ_0 is obtained in an SCF Hartree–Fock calculation and the excited target wavefunction φ_1 is built from the frozen-core orbitals of the initial target state except that the excited electron orbital is obtained by diagonalizing the V^{N-1} potential (Hunt and Goddard 1974). These distorted wavefunctions are solutions of the Lippmann–Schwinger equation

$$\chi_{\boldsymbol{k}}^{\pm} = \Phi_{\boldsymbol{k}} + G_0^{\pm} U_1 \chi_{\boldsymbol{k}}^{\pm} \tag{9}$$

with $G_0^{\pm}$ being the free-particle Green's operator with outgoing- (G_0^+) or incoming-wave (G_0^-) boundary conditions, and $\Phi_{\boldsymbol{k}}$ the plane wavefunction, with linear momentum $\boldsymbol{k}$. Equation (9) is solved using the Schwinger variational iterative method (SVIM) (Lucchese *et al* 1982) where the distorted wavefunctions χ's are kept orthogonal to the occupied orbitals of φ_0. In the SVIM calculations, the continuum wavefunctions are single-centre expanded as

$$\chi_{\boldsymbol{k}}(\boldsymbol{r}) = \left(\frac{2}{\pi}\right)^{1/2} \sum_{lm} \frac{(\mathrm{i})^l}{k} \chi_{klm}(\boldsymbol{r}) Y_{lm}(\hat{k}) \tag{10}$$

where $Y_{lm}(\hat{k})$ are the usual spherical harmonics. The calculation of $\chi_k(\boldsymbol{r})$ starts with the expansion of the trial functions in a set R_0 of L^2 basis functions $\alpha_i(\boldsymbol{r})$ as follows:

$$\tilde{\chi}_{klm}(\boldsymbol{r}) = \sum_{i=1}^{N} a_{i,lm}(k)\alpha_i(\boldsymbol{r}) \,. \tag{11}$$

Using this basis set, the reactance K-matrix elements can be derived as

$$K_{kll'm}^{(R_0)} = \sum_{i,j=1}^{N} \langle \Phi_{k,l'm} \mid U_1 \mid \alpha_i \rangle [D^{-1}]_{ij} \langle \alpha_j \mid U_1 \mid \Phi_{klm} \rangle \tag{12}$$

where

$$D_{ij} = \langle \alpha_i \mid U_1 - U_1 G_0^P U_1 \mid \alpha_j \rangle \,. \tag{13}$$

Here G_0^P is the principal-value free-particle Green's operator and the zeroth-iteration solution of equation (9), $\Psi_{klm}^{(R_0)}$, is obtained using equation (11) with appropriately calculated coefficients $a_{i,lm}$. The iterative procedure starts by augmenting R_0 by the set

$$S_0 = \{\chi_{k,l_1m_1}^{(R_0)}(\boldsymbol{r}), \chi_{k,l_2m_2}^{(R_0)}(\boldsymbol{r}), \ldots, \chi_{k,l_cm_c}^{(R_0)}(\boldsymbol{r})\} \tag{14}$$

where l_c is the maximum value of l for which the expansion of the scattering solution (10) is truncated, and $m_c \leqslant 2$. A new set of partial-wave scattering solutions is given by

$$\chi_{k,lm}^{P^{(R_1)}}(\boldsymbol{r}) = \Phi_{k,lm}(\boldsymbol{r}) + \sum_{i,j=1}^{M} \langle \boldsymbol{r} \mid G_0^P U_1 \mid \eta_i^{(R_1)} \rangle [D^{-1}]_{ij} \langle \eta_j^{(R_1)} \mid U_1 \mid \Phi_{k,lm} \rangle \tag{15}$$

where $\eta_i^{(R_1)}(\boldsymbol{r})$ is any function in the set $R_1 = R_0 \bigcup S_0$ and M is the number of functions in R_1. This iterative procedure continues until a converged $\chi_{k,lm}^{P^{(R_n)}}(\boldsymbol{r})$ is achieved.

Using the converged distorted wavefunctions, the T-matrix can be partial-wave expanded as

$$T_{fi} = \left(\frac{2}{\pi}\right) \sum_{lm} \sum_{l'm'} \frac{\mathrm{i}^{l-l'}}{k_i k_f} T_{lml'm'} Y_{lm}^*(\hat{k}_i) Y_{l'm'}(\hat{k}_f) \tag{16}$$

where $T_{lml'm'}$ is the partial-wave T-matrix element given by

$$T_{lml'm'} = \langle \varphi_1 \chi_{k_f,l'm'}^- \mid U \mid \varphi_0 \chi_{k_i,lm}^+ \rangle \,. \tag{17}$$

The LF scattering amplitude given in equation (1) can be expanded in a j_t-basis (Fano and Dill 1972) as

$$f(\hat{k}_f') = \sum_{j_t m_t m_t'} B_{m_t m_t'}^{j_t}(\hat{k}_f') D_{m_t m_t'}^{j_t}(\alpha, \beta, \gamma) \tag{18}$$

where $D_{m_t m_t'}^{j_t}(\alpha, \beta, \gamma)$ are the usual rotation matrices (Edmonds 1974), $\boldsymbol{j}_t = \boldsymbol{l}' - \boldsymbol{l}$ is the angular momentum transferred during the collision, and m_t', m_t are the projections of j_t along the laboratory and molecular axes, respectively. The expansion coefficient $B_{m_t m_t'}^{j_t}(\hat{k}_f')$ can be expressed as

$$B_{m_t m_t'}^{j_t}(\hat{k}_f') = \sum_{l'lm'm} (-1)^m a_{ll'mm'} (ll'0m_t \mid j_t m_t)(ll'mm' \mid j_t m_t') Y_{lm_l}(\hat{k}_f') \tag{19}$$

where the dynamical coefficients $a_{ll'mm'}$ for the transition from a initial target state $|i\rangle$ to a final target state $|f\rangle$ can be written in terms of fixed-nuclei partial-wave components of the electronic portion of the transition matrix elements as

$$a_{ll'mm'}(f \leftarrow i) = -\left(\frac{\pi}{2}\right) [4\pi(2l'+1)]^{1/2} \mathrm{i}^{l'-l} T_{lml'm'} \,. \tag{20}$$

After substituting equation (18) in equation (1) and performing the angular integrations, the LF DCS represented in a j_t-basis can be written as

$$\frac{\mathrm{d}\sigma}{\mathrm{d}\Omega}(f \leftarrow i) = SM_f \frac{k_f}{k_i} \sum_{j_t m_t m_t'} \frac{1}{(2j_t+1)} |B^{j_t}_{m_t m_t'}(f \leftarrow i, k_i, k_f, \hat{r'})|^2 . \tag{21}$$

For transitions leading to triplet excited states, only the exchange part of the T-matrix is needed. The cross sections are calculated via equations (19)–(21), where the summation in equation (19) is truncated at some cut-off values (l_c, m_c), appropriately chosen to ensure convergence. For transitions leading to singlet excited states, however, the convergence of the partial-wave expansion of the transition matrices is usually slow. In this case, although the partial-wave expansion of the DWA transition T-matrix is also truncated at some parameters (l_c, m_c), contributions from higher partial waves are accounted for via a Born-closure procedure. In this procedure, the Born-corrected expansion coefficients $B^{j_t}_{m_t m_t'}$ are given by

$$B^{j_t}_{m_t m_t'}(\hat{k_f'}) = B^{\mathrm{Born},\, j_t}_{m_t m_t'}(\hat{k_f'}) + \sum_{l' l m m'} (-1)^m (\mathrm{i})^{l-l'} (2l+1)^{-1} (T_{ll'mm'} - T^{\mathrm{Born}}_{ll'mm'}) \times (l-m, l'm' \mid j_t' m_t')(l0, l'm_t \mid j_t m_t) Y_{l'm_t}(\hat{k_f'}) \tag{22}$$

where $B^{\mathrm{Born},\, j_t}_{m_t m_t'}(\hat{k_f'})$ are the expansion coefficients in a j_t-basis representation of the Born scattering amplitude (as in equation (18)), and $T^{\mathrm{Born}}_{ll'mm'}$ is the partial-wave Born T-matrix element given by

$$T^{\mathrm{Born}}_{ll'mm'} = \langle S_{klm} \mid U_{st} \mid S_{kl'm'} \rangle \tag{23}$$

where U_{st} is twice the static potential (in atomic units) and S_{klm} are the partial-wave components of the free-particle wavefunction.

3. Computational details

In the DWA, the initial and the final wavefunctions of the scattered electron, needed for the computation of the T-matrix, were obtained in the ground-state molecular potential field at the static-exchange level. The target ground-state wavefunction was calculated using the Hartree–Fock–Roothaan approximation. The basis set used for this calculation is listed in table 1. With this basis set, at the equilibrium geometry ($R_{\mathrm{C-O}}$ = 2.132 au), the obtained SCF total energy and dipole moment are −112.776 au and −0.104 au, respectively, which compare well with the corresponding Hartree–Fock limits of −112.786 au and −0.108 au (Huo 1965). The same basis set was also used to calculate the wavefunctions of the excited states using the improved virtual orbital (IVO) approximation (Hunt and Goddard 1974). The calculated vertical excitation energies for the transitions to a $^3\Pi$, A $^1\Pi$, b $^3\Sigma^+$ and B $^1\Sigma^+$ states at the equilibrium geometry of the ground state are 6.00, 9.52, 11.15 and 12.05 eV, respectively, which can be compared with the experimental values 6.01, 8.03, 10.39 and 10.78 eV of Middleton *et al* (1993) measured from the $v = 0$ vibrational level of the ground state to the $v' = 0$ vibrational level of the excited states. Our calculated vertical excitation energies are also in good agreement with those calculated by Sun *et al* (1992) and by Weatherford and Huo (1990).

Both the incident- and the scattered-electron distorted continuum wavefunctions were truncated at $l_c = 20$ and $m_c = 2$. The distorted-wave T-matrix was also truncated using the same parameters. Unperturbed plane wavefunctions were used to calculate the partial-wave T-matrix elements corresponding to $m \geqslant 3$, for transitions leading to triplet excited states.

Table 1. Cartesian Gaussian functions[a] used in the SCF calculations.

	s		p		d	
Atom	Exp.	Coeff.	Exp.	Coeff.	Exp.	Coeff.
C	4232.61	0.006 228	18.155 7	0.039 196		
	634.882	0.047 676	3.986 40	0.244 144		
	146.097	0.231 439	1.142 90	0.816 775		
	42.497 4	0.789 108				
	14.189 2	0.791 751				
	1.966 60	0.321 870				
	5.147 70	1.000 000	0.359 40	1.000 000	1.500	1.000 000
	0.496 20	1.000 000	0.114 60	1.000 000	0.750	1.000 000
	0.153 30	1.000 000	0.045 84	1.000 000	0.300	1.000 000
	0.061 32	1.000 000	0.020 00	1.000 000		
	0.030 00	1.000 000				
	0.010 00	1.000 000				
	0.003 00	1.000 000				
O	7816.54	0.006 436	35.183 2	0.040 023		
	1175.82	0.048 924	7.904 00	0.253 849		
	273.188	0.233 819	2.305 10	0.806 842		
	81.169 6	0.784 798				
	27.183 6	0.803 381				
	3.413 60	0.316 720				
	9.532 20	1.000 000	0.717 10	1.000 000	1.700	1.000 000
	0.939 80	1.000 000	0.213 70	1.000 000	0.850	1.000 000
	0.284 60	1.000 000	0.085 48	1.000 000	0.340	1.000 000
	0.113 84	1.000 000	0.040 00	1.000 000		
	0.050 00	1.000 000				
	0.020 00	1.000 000				
	0.005 00	1.000 000				

[a] Cartesian Gaussian basis functions are defined as

$$\phi^{\alpha,\ell,m,n,\boldsymbol{A}}(\boldsymbol{r}) = N(x-\boldsymbol{A}_x)^{\ell}(y-\boldsymbol{A}_y)^{m}(z-\boldsymbol{A}_z)^{n}\exp(-\alpha|\boldsymbol{r}-\boldsymbol{A}|^2)$$

with N a normalization constant.

A test of convergence was carried out and showed that the DCS for this type of transition converge to better than 2% using $m_c = 5$ for incident energies up to 50 eV. At higher energies $m_c = 8$ is needed. In table 2 we show the basis set R_0 used for the calculation of the initial trial scattering functions. All calculations were converged within three iterations.

Table 2. Basis set used for the initial scattering functions.

Scattering symmetry	Atom	Type of Cartesian Gaussian function	Exponents
$k\sigma$	C	s	8.0, 4.0, 2.0, 1.0, 0.5, 0.2
		z	4.0, 2.0, 1.0, 0.3
$k\pi, k\delta$	C	x	8.0, 4.0, 2.0, 1.0, 0.5, 0.2
		xz	4.0, 2.0, 1.0, 0.3
$k\sigma$	O	s	8.0, 4.0, 2.0, 1.0, 0.5, 0.2
		z	4.0, 2.0, 1.0, 0.3
$k\pi, k\delta$	O	x	8.0, 4.0, 2.0, 1.0, 0.5, 0.2
		xz	4.0, 2.0, 1.0, 0.3

4. Results and discussion

4.1. $a^3\Pi$ state

Figures 1(*a*)–(*f*) show our DWA DCS for the X $^1\Sigma \rightarrow$ a $^3\Pi$ transition in CO at 20, 30, 40, 50, 80 and 100 eV, respectively, along with the experimental data of Trajmar *et al* (1971), Cartwright and Trajmar (1981) and Middleton (1994). The calculated DWA results of Lee and McKoy (1982) at 20 and 50 eV and the SMC results of Sun *et al* (1992) at 20 and 30 eV are also shown. In general, there is a qualitative agreement between our calculated results and the experimental data of Middleton (1994) at incident energies where the comparison is possible. Quantitatively, the agreement between our results and the experimental data of

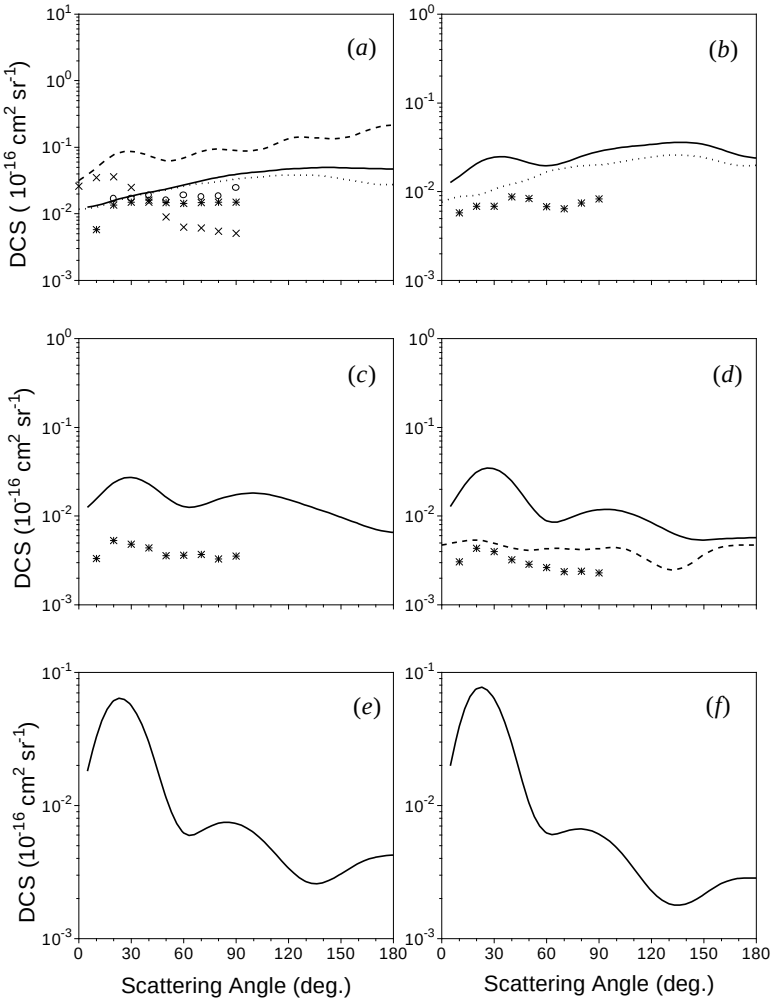

Figure 1. DCS for the X $^1\Sigma \rightarrow$ a $^3\Pi$ transition in CO at (*a*) 20, (*b*) 30, (*c*) 40, (*d*) 50, (*e*) 80 and (*f*) 100 eV. Full curve, present DWA results; short-broken curve, five-state SMC results of Sun *et al* (1992); long-broken curve, earlier DWA results of Lee and McKoy (1982); crosses, experimental data of Trajmar *et al* (1971); open circles, experimental data of Cartwright and Trajmar (1981); asterisks, experimental data of Middleton (1994).

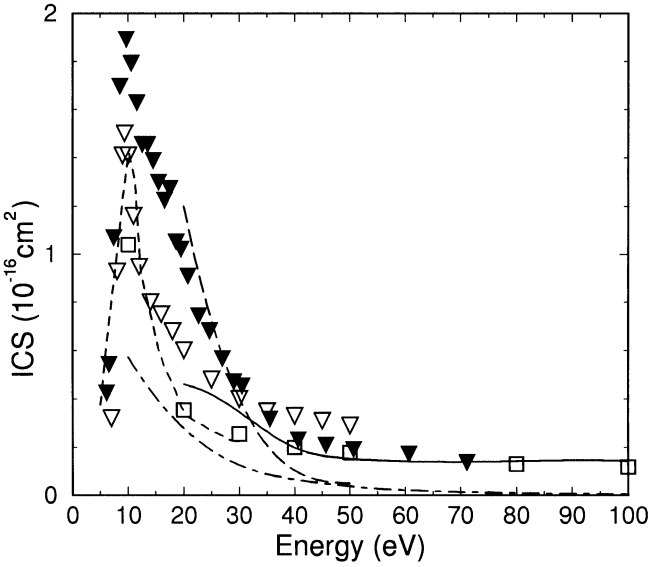

Figure 2. ICS for the electron-impact excitation X $^1\Sigma \rightarrow$ a $^3\Pi$ in CO in the 20–100 eV range. Full curve, present DWA results; short-broken curve, five-state SMC results of Sun *et al* (1992); long-broken curve, earlier DWA results of Lee and McKoy (1982); chain curve, Born–Rudge theoretical results of Chung and Lin (1974); open squares, relative experimental data of Ajello (1971); inverted full triangles, absolute measurements of Furlong and Newell (1996); inverted open triangles, relative data of LeClair *et al* (1994).

Table 3. DCS and ICS (in 10^{-18} cm^2) for the X $^1\Sigma \rightarrow$ a $^3\Pi$ excitation in CO.

Angle	E_0 (eV)					
(deg)	20	30	40	50	80	100
10	1.33	1.48	1.56	1.83	3.27	3.95
20	1.58	2.07	2.38	3.14	6.15	7.51
30	1.86	2.45	2.71	3.42	5.64	6.33
40	2.10	2.39	2.29	2.47	2.96	2.91
50	2.36	2.10	1.63	1.37	1.14	1.04
60	2.70	1.96	1.28	0.884	0.620	0.619
70	3.11	2.13	1.31	0.902	0.644	0.637
80	3.54	2.49	1.54	1.07	0.734	0.669
90	3.91	2.83	1.74	1.17	0.730	0.610
100	4.22	3.08	1.81	1.16	0.624	0.482
110	4.48	3.25	1.72	1.03	0.470	0.336
120	4.71	3.42	1.54	0.845	0.337	0.228
130	4.88	3.57	1.32	0.666	0.268	0.182
140	4.97	3.60	1.13	0.563	0.263	0.182
150	4.95	3.40	0.968	0.538	0.306	0.214
160	4.87	2.99	0.818	0.550	0.368	0.260
170	4.78	2.58	0.703	0.564	0.410	0.282
180	4.74	2.41	0.658	0.569	0.423	0.286
ICS	46.0	34.7	19.9	15.2	14.2	14.2

Cartwright and Trajmar (1981) and of Middleton (1994) is fair at 20 eV. At higher energies, however, our calculation overestimates the DCS. At 20 eV (figure 1(*a*)) our DCS are in

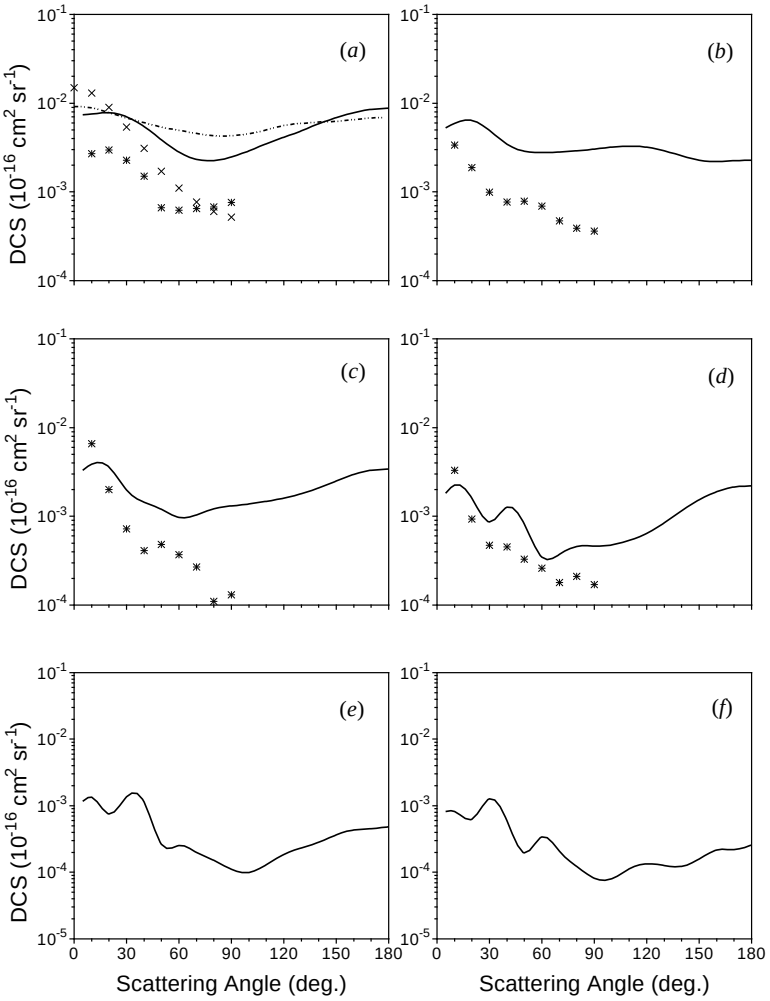

Figure 3. Same as figure 1 for the X $^1\Sigma \rightarrow$ b $^3\Sigma^+$ excitation except: chain curve, two-state SMC results of Weatherford and Huo (1990).

very good agreement, both qualitatively and quantitatively, with the five-state SMC data of Sun *et al* (1992). Nevertheless, the results of Lee and McKoy (1982) are systematically larger than ours by a factor of three and show some oscillations. We believe that the large discrepancy between these two DWA calculations is mainly due to the description of the target wavefunctions. In contrast to the present study, neither d-type functions nor diffuse basis functions were included in their calculations. In addition, this discrepancy can also be partly attributed to different truncation parameters used in both calculations: ($l_c = 20$, $m_c = 5$) in ours and ($l_c = 10$, $m_c = 2$) in theirs, which suggests that their T-matrix partial-wave expansion was possibly not fully converged. At 30 eV (figure 1(b)), our DWA results agree with the SMC results within 30%. This difference could be partly due to the different truncation of the m_c parameter used in both calculations: $m_c = 5$ in ours and $m_c = 2$ in theirs, for this energy. At 50 eV (figure 1(d)), the earlier DWA results of Lee and McKoy are systematically lower than ours. Again, different truncation parameters

Table 4. DCS and ICS (in 10^{-18} cm^2) for the X $^1\Sigma \rightarrow$ b $^3\Sigma^+$ excitation in CO.

Angle (deg)	E_0 (eV)					
	20	30	40	50	80	100
10	0.759	0.589	0.385	0.224	0.134	0.082
20	0.783	0.637	0.359	0.161	0.076	0.062
30	0.703	0.491	0.199	0.086	0.136	0.127
40	0.543	0.342	0.144	0.126	0.113	0.059
50	0.386	0.286	0.119	0.081	0.026	0.020
60	0.282	0.277	0.097	0.035	0.025	0.034
70	0.232	0.282	0.103	0.037	0.020	0.021
80	0.225	0.291	0.120	0.046	0.015	0.012
90	0.247	0.304	0.130	0.046	0.011	0.008
100	0.290	0.319	0.137	0.047	0.010	0.008
110	0.346	0.327	0.147	0.054	0.013	0.011
120	0.412	0.318	0.160	0.064	0.018	0.013
130	0.491	0.290	0.179	0.084	0.023	0.013
140	0.583	0.255	0.209	0.115	0.028	0.012
150	0.684	0.228	0.250	0.153	0.037	0.016
160	0.780	0.220	0.295	0.189	0.043	0.022
170	0.849	0.224	0.329	0.212	0.045	0.022
180	0.875	0.227	0.341	0.220	0.049	0.026
ICS	5.29	3.97	2.06	0.995	0.432	0.322

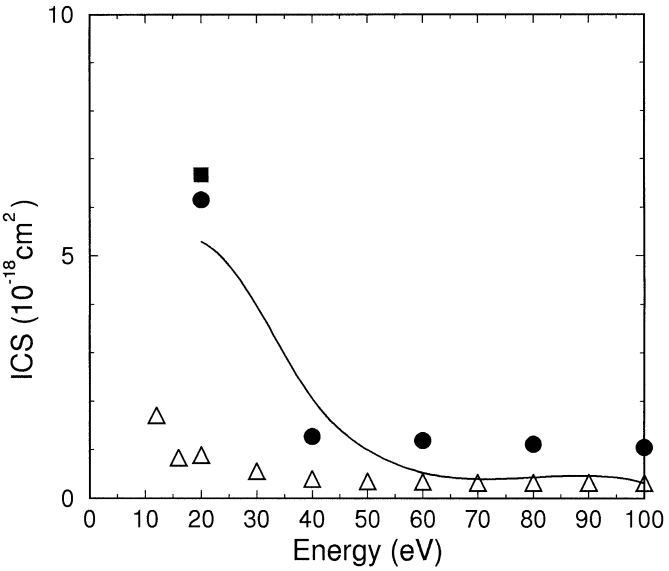

Figure 4. ICS for the X $^1\Sigma \rightarrow$ b $^3\Sigma^+$ excitation in CO in the 20–100 eV region. Full curve, present DWA results; full squares, two-state SMC results of Weatherford and Huo (1990); open triangles, experimental data of Skubenich (1967); full circles, experimental data of Land (1978).

used in both DWA calculations could be the reason for this disagreement. Thus, the good agreement between the calculated DCS (Lee and McKoy 1982) and the experimental data of Middleton (1994) may be fortuitous. For incident energies above 50 eV, there are neither

experimental nor theoretical results reported in the literature for this transition. Therefore, we hope our results can serve for comparison in future investigations. The oscillations in the DCS are noticed to increase with increasing incident energies. This behaviour was also observed for the same type of transitions in other molecules (Lee *et al* 1995).

In figure 2 we present our calculated ICS for the X $^1\Sigma \rightarrow$ a $^3\Pi$ transition in CO in the 20–100 eV range along with the relative experimental data of Ajello *et al* (1971), normalized to our results at 40 eV, the relative experimental data of LeClair *et al* (1994) normalized to the maximum cross sections reported by Erdman and Zipf (1983) and the recent absolute measurements of Furlong and Newell (1996). The theoretical results obtained by using the five-state SMC (Sun *et al* 1992), the DWA (Lee and McKoy 1982) and the Born–Rudge (BR) approximation (Chung and Lin 1974) are also shown. All the calculated ICS agree qualitatively with the experimental data . Above 30 eV, our calculated ICS are in very good agreement with the absolute ICS of Furlong and Newell. In the 20–30 eV range, the SMC results of Sun *et al* are about 30% lower than ours. The BR ICS of Chung and Lin are systematically lower, whereas the DWA ICS of Lee and McKoy are larger than our data at lower incident energies but smaller than ours at higher incident energies.

Table 5. DCS and ICS (in 10^{-18} cm^2) for the X $^1\Sigma^+ \rightarrow$ A $^1\Pi$ excitation in CO.

Angle	E_0 (eV)					
(deg)	20	30	40	50	80	100
10	77.9	177.0	209.0	208.0	164.0	133.0
20	37.2	53.2	47.9	39.1	23.3	16.4
30	17.7	18.5	14.5	11.2	5.91	4.12
40	10.1	8.61	6.50	5.10	2.66	1.92
50	7.50	5.75	4.36	3.16	1.57	1.10
60	6.66	4.95	3.57	2.31	1.06	0.747
70	6.41	4.70	3.05	1.86	0.827	0.602
80	6.22	4.53	2.68	1.64	0.723	0.516
90	5.88	4.29	2.50	1.63	0.715	0.467
100	5.39	4.03	2.51	1.77	0.783	0.483
110	4.83	3.87	2.67	1.95	0.899	0.561
120	4.28	3.87	2.93	2.17	1.05	0.691
130	3.75	3.95	3.21	2.43	1.28	0.878
140	3.20	3.86	3.45	2.78	1.56	1.10
150	2.60	3.45	3.63	3.21	1.85	1.32
160	2.00	2.77	3.76	3.70	2.09	1.49
170	1.54	2.15	3.86	4.12	2.25	1.61
180	1.36	1.89	3.89	4.29	2.31	1.66
ICS	102	122	117	108	83.9	69.7

4.2. b $^3\Sigma^+$ state

In figures 3(*a*)–(*f*) we show our DWA DCS for the X $^1\Sigma \rightarrow$ b $^3\Sigma^+$ transition in CO at 20, 30, 40, 50, 80 and 100 eV, respectively. The experimental data of Trajmar *et al* (1971) at 20 eV (figure 3(*a*)), of Middleton (1994) in the 20–50 eV range and the calculated two-state SMC results of Weatherford and Huo (1990) are also shown. There is a qualitative agreement between our calculated results and the experimental data at 20 and 50 eV. Quantitatively, our DCS are overestimated in comparison with the measured data for all energies, except

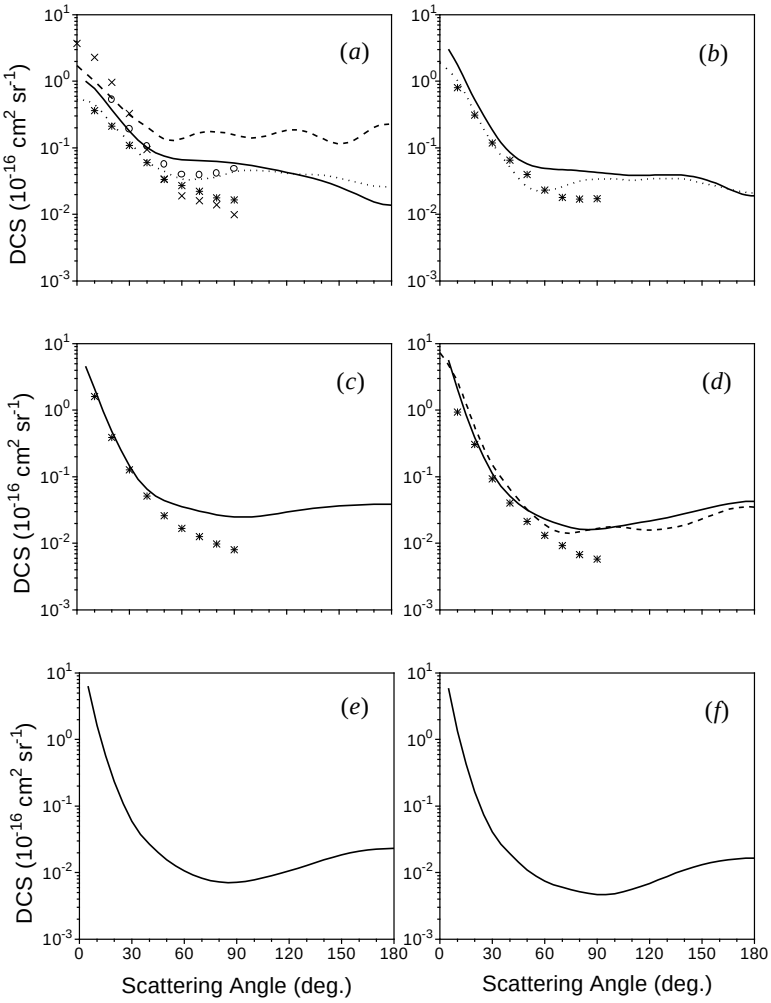

Figure 5. Same as figure 1 for the X $^1\Sigma \rightarrow$ A $^1\Pi$ excitation.

at small scattering angles. At 20 eV, the two-state SMC cross sections of Weatherford and Huo are nearly isotropic, whereas our results exhibit a minimum at around 80°. As in the X $^1\Sigma \rightarrow$ a $^3\Pi$ case, it can also be noticed that the oscillations in the DCS increase with increasing incident energies.

Figure 4 shows our DWA ICS for the X $^1\Sigma \rightarrow$ b $^3\Sigma^+$ transition in CO by electron impact in the 20–100 eV energy range along with the experimental data of Land (1978) and of Skubenich (1967), and the calculated two-state SMC ICS of Weatherford and Huo at 20 eV. In general, our results agree well with the measured data of Land (1978) and quite well with those of Skubenich for incident energies above 60 eV. The two-state SMC ICS at 20 eV is about 25% larger than ours. On the other hand the BO results (not shown) of Chung and Lin are systematically much lower than our data.

4.3. A $^1\Pi$ state

Figures 5(*a*)–(*f*) compare the DWA DCS for the X $^1\Sigma \rightarrow$ A $^1\Pi$ transition in CO with the experimental data of Trajmar *et al* (1971), of Cartwright and Trajmar (1981) and of Middleton (1994), as well as with the DWA results of Lee and McKoy (1982) and with the five-state SMC results of Sun *et al* (1992). As expected, for this dipole-allowed transition the calculated DCS are, in general, strongly forward-peaked, in accordance with the measurements. Our DWA DCS are in general good agreement with the experimental data, particularly for small scattering angles. At lower energies, our results agree very well with the experimental data of Cartwright and Trajmar, and also with the five-state SMC results of Sun *et al*. At 50 eV (figure 5(*d*)) the earlier DWA DCS of Lee and McKoy are in very good agreement with our calculations. However, their DCS at 20 eV were systematically larger than ours and exhibit some oscillations. Again, these discrepancies can possibly be attributed to different target wavefunctions used in both calculations.

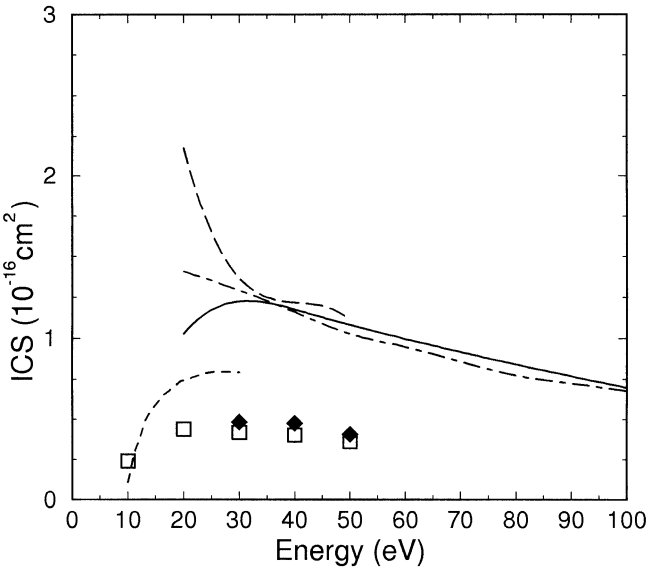

Figure 6. Same as figure 2 for the X $^1\Sigma \rightarrow$ A $^1\Pi$ excitation except: full diamonds, experimental data of Mumma *et al* (1971).

Figure 6 compares our DWA ICS for this transition with the experimental values of Ajello (1971) and Mumma *et al* (1971), both obtained by a radiation-emission technique, as well as with the five-state SMC ICS of Sun *et al*, the DWA ICS of Lee and McKoy and the Born–Ochkur (BO) ICS of Chung and Lin. All the theories overestimate the ICS and the five-state SMC shows the best agreement with the experiments. Our DWA ICS are larger than the experimental results by a factor of 3 and are about 1.5 times larger than the SMC ICS. At 30 eV and above, the DWA ICS of Lee and McKoy, as well as the BO ICS (Chung and Lin 1974), agree very well with the present calculations.

4.4. B $^1\Sigma^+$ state

In figures 7(*a*)–(*f*) we show our DWA DCS for the X $^1\Sigma \rightarrow$ B $^1\Sigma^+$ transition in CO at 20, 30, 40, 50, 80 and 100 eV, respectively. The experimental data of Trajmar *et al* (1971)

at 20 eV, of Middleton *et al* (1994) in the 20–50 eV range and of Kanik *et al* (1993) at 100 eV are also shown. There are no reported theoretical data for this transition. In general, our DWA DCS are in quite good agreement with the measured data of Middleton at small scattering angles. For angles $\geqslant 60^{\circ}$, our method overestimates the DCS. However, the agreement with the experimental data of Middleton improves with the increase of incident energies. At 20 eV (figure 7(*a*)), the experimental data of Trajmar *et al* strongly disagree with our results. On the other hand, at 100 eV (figure 7(*f*)), our results agree fairly well with the experimental results of Kanik *et al*.

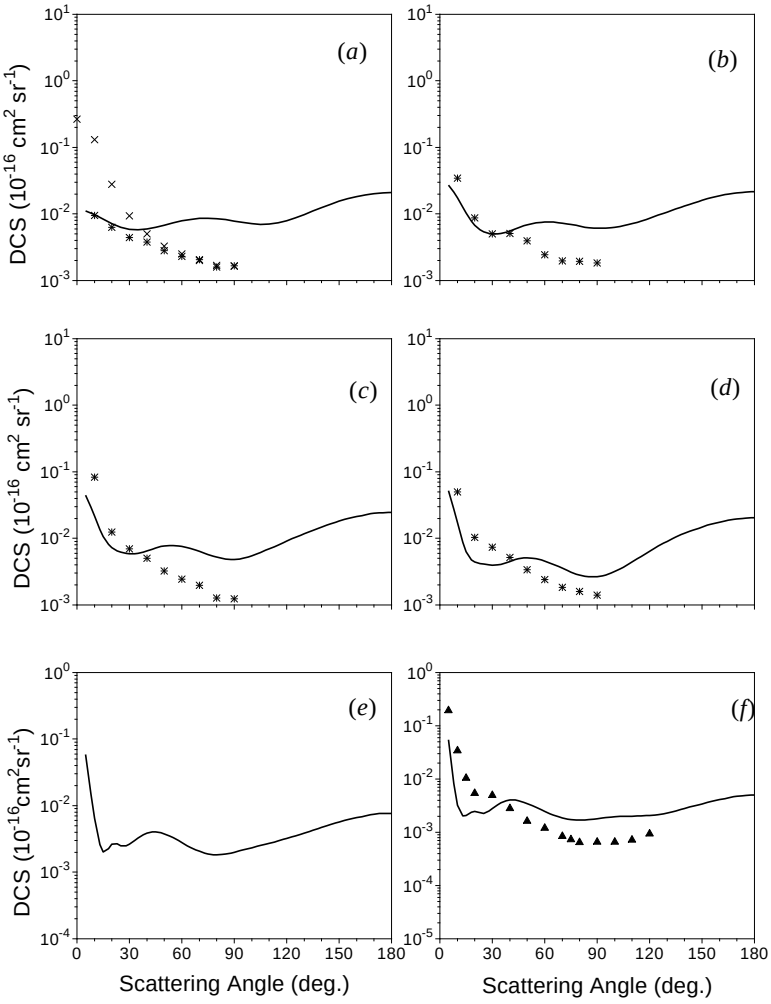

Figure 7. Same as figure 1 for the X $^1\Sigma \rightarrow$ B $^1\Sigma^+$ excitation except: full triangles, experimental data of Kanik *et al* (1993).

Figure 8 shows our calculated ICS for the X $^1\Sigma \rightarrow$ B $^1\Sigma^+$ transition in the 20–100 eV range in comparison with the BO ICS of Chung and Lin. The experimental results of Aarts and de Heer (1970) and of Kanik *et al*, both at 100 eV, and those of Skubenich (1967) in the 20–100 eV range are also shown. Our ICS show a broad resonance-like feature at about 40 eV. No such feature is seen in the BO study for this transition. However, for

Table 6. DCS and ICS (in 10^{-18} cm^2) for the X $^1\Sigma^+ \rightarrow$ B $^1\Sigma^+$ excitation in CO.

Angle (deg)	E_0 (eV)					
	20	30	40	50	80	100
10	0.981	1.74	2.15	1.71	0.646	0.323
20	0.712	0.680	0.725	0.441	0.263	0.245
30	0.588	0.501	0.588	0.394	0.264	0.279
40	0.592	0.557	0.649	0.451	0.385	0.402
50	0.677	0.688	0.766	0.509	0.376	0.347
60	0.787	0.760	0.758	0.457	0.280	0.244
70	0.856	0.729	0.640	0.356	0.206	0.185
80	0.848	0.655	0.522	0.281	0.183	0.170
90	0.783	0.610	0.484	0.265	0.199	0.180
100	0.716	0.630	0.546	0.317	0.233	0.194
110	0.706	0.718	0.695	0.441	0.272	0.200
120	0.793	0.866	0.910	0.640	0.320	0.206
130	0.983	1.06	1.17	0.902	0.388	0.231
140	1.25	1.31	1.48	1.19	0.473	0.278
150	1.55	1.60	1.81	1.48	0.568	0.341
160	1.83	1.88	2.13	1.75	0.662	0.411
170	2.02	2.08	2.37	1.96	0.738	0.472
180	2.09	2.16	2.46	2.04	0.769	0.498
ICS	11.1	10.8	11.2	7.91	4.36	3.44

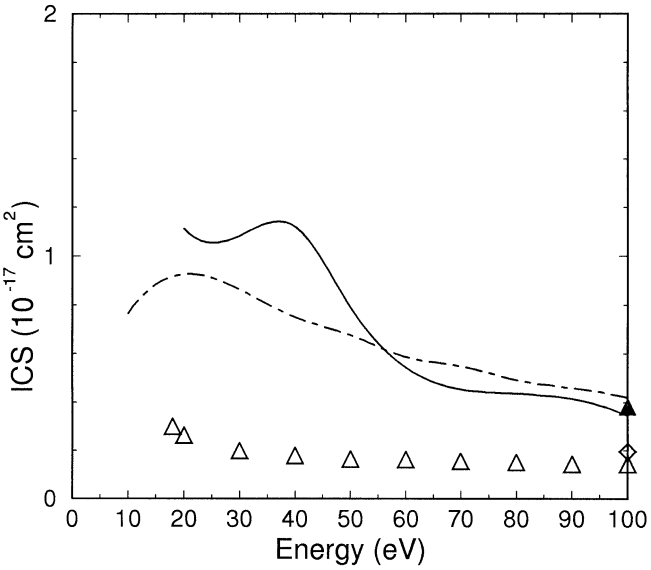

Figure 8. ICS for the X $^1\Sigma \rightarrow$ B $^1\Sigma^+$ excitation in CO in the 20–100 eV region. Full curve, present DWA results; chain curve, Born–Ochkur theoretical results of Chung and Lin (1974); open triangles, experimental data of Skubenich (1967); open diamond, experimental data of Aarts and de Heer (1970); full triangle, experimental result of Kanik *et al* (1993).

incident energies above 50 eV, there is a quite good agreement between our DWA ICS and the BO results. At 100 eV, both theories agree very well with the experimental data of

Kanik *et al*, while the result of Aarts and de Heer is about half of our calculated value. The experimental data of Skubenich lie systematically below the calculated results.

The numerical values of the calculated DCS and ICS for all the transitions studied herein are shown in tables 3–6.

5. Conclusions

In this work we report a DWA study of the electronic transitions leading to the a $^3\Pi$, b $^3\Sigma^+$, A $^1\Pi$ and B $^1\Sigma^+$ states from the ground state of the CO molecule by electron impact in the 20–100 eV range. Our calculated DCS and ICS are compared with the available experimental and theoretical data. In general, our DWA DCS and ICS are in good agreement with the five-state SMC data of Sun *et al* (1992) for the X $\rightarrow$ a and X $\rightarrow$ A transitions and with the two-state SMC results of Weatherford and Huo (1990) for the X $\rightarrow$ b transition. Considering the computational simplicity of the DWA in comparison with the usual multichannel methods, the application of that approximation as a first study of electron-impact molecular excitation is clearly of interest. The comparison between our DWA results and those of Lee and McKoy (1982), also obtained using the DWA, shows significant influence of the description of the target wavefunction in the calculation of cross sections, particularly at low incident energies. Our calculated DCS and ICS are generally in good qualitative agreement with the available experimental data. Quantitatively, our method overestimates the cross sections. It is interesting to note that the comparison of our results to various other calculations is better than the comparison to the experimental data. This is probably due to the fact that all the reported calculations neglect the electronic correlation in the target states. Finally, due to the scarcity of reported experimental data and sometimes to serious discrepancies among various measurements, additional experimental studies for such processes are desirable for a better evaluation of the theoretical methods.

Acknowledgments

This research was partially supported by the Brazilian Agencies Conselho Nacional de Desenvolvimento Científico e Tecnológico (CNPq), FAPESP and FINEP-PADCT. Two of us (AMM and MMF) thank FAPESP for scholarships.

References

Aarts J F M and de Heer F J 1970 *J. Chem. Phys.* **52** 5354
Ajello J M 1971 *J. Chem. Phys.* **55** 3158
Bartschat K and Madison D H 1987 *J. Phys. B: At. Mol. Phys.* **20** 5839
Cartwright D C and Kuppermann A 1967 *Phys. Rev* **163** 86
Cartwright D C and Trajmar S 1981 as quoted by Lee and McKoy (1982)
Chung S and Lin C C 1974 *Phys. Rev.* A **9** 1954
Chung S, Lin C C and Lee E T P 1975 *Phys. Rev.* A **12** 1340
Collins L A and Schneider B I 1990 *Electronic and Atomic Collisions* ed H B Gilbody, W R Newell, F H Read and A C H Smith (Amsterdam: Elsevier)
Cooper D L and Kirby K 1987 *J. Chem. Phys.* **87** 424
Edmonds A R 1974 *Angular Momentum in Quantum Mechanics* (Princeton, NJ: Princeton University Press)
Erdman P W and Zipf E C 1983 *Planet. Space Sci.* **31** 317
Fano U and Dill D 1972 *Phys. Rev.* A **6** 185
Fliflet A W and McKoy V 1980 *Phys. Rev.* A **21** 1863
Fox J L and Dalgarno A 1979 *J. Geophys. Res.* **84** 7315
Furlong J M and Newell W R 1996 *J. Phys. B: At. Mol. Opt. Phys.* **29** 331

Hazi A U 1981 *Phys. Rev.* A **23** 2232
Hunt W J and Goddard W A III 1974 *Chem. Phys. Lett.* **24** 464
Huo W M 1965 *J. Phys. Phys.* **43** 624
Kanik I, Ratliff M and Trajmar S 1993 *Chem. Phys. Lett.* **208** 321
Land J E 1978 *J. Appl. Phys.* **49** 5716
LeClair L R, Brown M D and McConkey J W 1994 *Chem. Phys.* **189** 769
Lee M-T, Brescansin L M and Lima M A P 1990a *J. Phys. B: At. Mol. Opt. Phys.* **23** 3859
Lee M-T and McKoy V 1982 *J. Phys. B: At. Mol. Phys.* **15** 3971
Lee M-T, Machado L E, Brescansin L M and Meneses G D 1991 *J. Phys. B: At. Mol. Opt. Phys.* **24** 509
Lee M-T, Machado L E, Leal E P, Brescansin L M, Lima M A P and Machado F B C 1990b *J. Phys. B: At. Mol. Opt. Phys.* **23** L233
Lee M-T, Michelin S E, Kroin T, Machado, L E and Brescansin L M 1995 *J. Phys. B: At. Mol. Opt. Phys.* **28** 1859
Lee M-T, Michelin S E, Machado L E and Brescansin L M 1993 *J. Phys. B: At. Mol. Opt. Phys.* **26** L203
Lee M-T, Taveira A M A, Fujimoto M M, Machado L E and Brescansin L M 1996 *J. Mol. Struct. (Theochem.)* at press
McDaniel E W and Nighan W L 1982 *Applied Atomic Collision Physics* vol 3 *Gas Lasers* (New York: Academic) p 118
Lucchese R R, Raseev G and McKoy V 1982 *Phys. Rev.* A **25** 2572
Meneses G D, Pagan C B and Machado L E 1990 *Phys. Rev.* A **41** 4740
Middleton A G 1994 *PhD Thesis* The Flinders University of Australia
Middleton A G, Brunger M J and Teubner P J O 1993 *J. Phys. B: At. Mol. Opt. Phys.* **26** 1743
Morgan L A and Tennyson J 1993 *J. Phys. B: At. Mol. Opt. Phys.* **26** 2429
Mumma M J, Stone E J and Zipf E C 1971 *J. Chem. Phys.* **54** 2627
Rescigno T N, McCurdy C W and McKoy V 1974 *J. Phys. B: At. Mol. Phys.* **7** 2396
Skubenich V V 1967 *Opt. Spektrosk.* **23** 990 (Engl. transl. 1967 *Opt. Spectrosc.* **23** 540)
Sun Q, Winstead C and McKoy V 1992 *Phys. Rev.* A **46** 6987
Trajmar S, Williams W and Cartwright D C 1971 *Proc. 7th Int. Conf. on Physics of Electronic and Atomic Collisions (Amsterdam)* Abstracts, p 1066
Trajmar S, Register D F and Chutjian A 1983 *Phys. Rep.* **97** 219
Weatherford C A and Huo W M 1990 *Phys. Rev.* A **41** 186